Article

Not peer-reviewed version

London Dispersive and Lewis Acid-Base Surface Energy of 2D Single-Crystalline and Polycrystalline Covalent Organic Frameworks

Tayssir Hamieh *

Posted Date: 22 January 2024

doi: 10.20944/preprints202401.1548.v1

Keywords: deformation polarizability; ionization energy; London dispersive free energy; polar energy of adsorption; Lewis's acid-base components of surface energy; molecular separation distance

Article

London Dispersive and Lewis Acid-Base Surface Energy of 2D Single-Crystalline and Polycrystalline Covalent Organic Frameworks

Tayssir Hamieh [1,2]

[1] Faculty of Science and Engineering, Maastricht University, P.O. Box 616, 6200 MD Maastricht, The Netherlands; t.hamieh@maastrichtuniversity.nl

[2] Laboratory of Materials, Catalysis, Environment and Analytical Methods Laboratory (MCEMA), Faculty of Sciences, Lebanese University, Hadath, Beirut, P.O. Box 6573/14 Badaro, Lebanon

Abstract: This paper is devoted to an accurate determination of the London dispersive and polar free energy of adsorption, the two Lewis acid γ_s^+ and base γ_s^- components of polar surface energy γ_s^{AB} of 2D single-crystalline and polycrystalline covalent organic frameworks such as TAPPy-TPA-COFs. Inverse gas chromatography (IGC) at infinite dilution was used to quantify the different surface parameters of the different materials. From IGC measurements, one determined the net retention time of the adsorption of n-alkanes and several polar solvents on single-crystalline and polycrystalline covalent organic frameworks. The free surface Gibbs energy of adsorption was obtained for the various organic molecules at different temperatures from their net retention volume values. The separation between the London dispersive energy and the polar energy of adsorbed molecules was carried out by using a new thermodynamic parameter $\mathcal{P}_{SX}$ chosen as new indicator variable and taken into account the deformation polarizability and the harmonic mean of the ionization energies of solvents and solid materials, derived from London dispersion equation. The obtained results are very promising for the accurate determination of the surface thermodynamic parameters of adsorption of organic solvents on solid surfaces.

Keywords: deformation polarizability; ionization energy; London dispersive free energy; polar energy of adsorption; Lewis's acid-base components of surface energy; molecular separation distance

1. Introduction

Covalent organic frameworks (COFs), discovered by Yaghi et al. [1] in 2005 are very interesting crystalline organic porous materials exhibiting very important surface properties concerning their large specific surface area, porosity [2]. Many research works on COFs and their synthesis were developed, due to their aptitude to be used as excellent materials in various applications such as catalysis [3–7], Rechargeable Batteries [8–10], separation processes [11], light-emitting materials [12], biomedicine, biosensors and bioelectronics [13,14].

Some promising covalent organic frameworks, such as two-dimensional 2D-COFs composed of 2D-layered polymers, exhibited excellent thermal conductivity [15] and heterogeneous catalytic activity [16]. Two-dimensional imine-based covalent organic framework, single-crystalline and polycrystalline TAPPy-TPA-COF synthetized from 4,4′,4″,4‴-(pyrene-1,3,6,8-tetrayl) tetraaniline (TAPPy) and terephthalaldehyde (TPA), were recently studied by several authors [17–22]. The physicochemical properties of 2D-COFs were studied by inverse gas chromatography at infinite dilution by Natraj et al. [18] and Yusuf et al. [19].

One proposed, in this paper, to determine the London dispersive, polar free energy, the two Lewis acid γ_s^+ and base γ_s^- components of polar surface energy γ_s^{AB} of 2D single-crystalline and polycrystalline covalent organic frameworks such as TAPPy-TPA-COFs. The used technique was the inverse gas chromatography (IGC) at infinite dilution [23–41] based on the experimental determination of the net retention time t_n and volume V_n of several organic molecules adsorbed on

 doi:10.20944/preprints202401.1548.v1

the solid materials. The fundamental thermodynamic equation of IGC allowing to obtain the free energy of adsorption ΔG_a^0 of any organic solvents on a solid surface was given in infinite dilution by the following equation:

$$\Delta G_a^0 = -RT\ lnV_n + RT\ ln\left(\frac{sm\pi_0}{P_0}\right) \quad (1)$$

where T is the absolute temperature of the chromatographic column containing the solid material, R the prefect gas constant, m is the mass of the solid material of a specific surface area s, and π_0 and P_0 are two reference characteristics respectively referred to the two-dimensional state and atmospheric pressure.

In the case of non-polar solvents such as n-alkanes, the only free energy of adsorption is that of the London dispersion component ΔG_a^d given by:

$$\Delta G_a^0 = \Delta G_a^d \quad (2)$$

For polar organic molecules, one has to add the specific free energy ΔG_a^{sp} of adsorption:

$$\Delta G_a^0 = \Delta G_a^d + \Delta G_a^{sp} \quad (3)$$

Many methods and models were proposed in literature [23–34] to determine ΔG_a^{sp} of polar solvents adsorbed on solid materials and the London dispersive surface energy γ_s^d of the studied materials. The values of ΔG_a^{sp} and γ_s^d obtained by the various chromatographic methods are very different and strongly depend on the used molecular model and IGC methods. In previous papers, one showed that the surface area of organic molecules not only depends on the chosen molecular surface areas of molecules but also on the temperature [32–37] and this affects the different surface thermodynamic parameters. On the other hand, even if we previously proposed the expressions of the surface area of organic molecules and corrected the calculation of γ_s^d of solids, the expressions of these surface areas cannot be always transferred to any other solid.

In a recent paper [42], one proposed a new method based on that of the London dispersion expression [43] by using a new thermodynamic parameter $\mathcal{P}_{SX}$ dependent both on the deformation polarizability α_{0X} of the probe and on the ionization energies of the solid ε_S and the solvent ε_X:

$$\mathcal{P}_{SX} = \frac{\varepsilon_S\,\varepsilon_X}{(\varepsilon_S + \varepsilon_X)}\alpha_{0X} \quad (4)$$

This method using the equation of the London dispersion interaction [43] was used to better quantify the different Lewis acid-base contributions of the surface energy single-crystalline and poly-crystalline TAPPy-TPA-COFs as well as their polar surface energy.

2. IGC Method and materials

The chromatographic measurements obtained in other studies [18,19,44] led to determine the free energy of adsorption ΔG_a^0 or $\boldsymbol{RTlnV_n}$ of the adsorbed molecules on the solid substrates as a function of the temperature. The proposed method is that using the deformation polarizability α_{0X} of the adsorbed molecule and the harmonic mean of the ionization energies, given by relation (5):

$$\Delta G_a^0(T) = -\frac{\alpha_{0S}}{H^6}\left[\frac{3\mathcal{N}}{2(4\pi\varepsilon_0)^2}\left(\frac{\varepsilon_S\,\varepsilon_X}{(\varepsilon_S + \varepsilon_X)}\alpha_{0X}\right)\right] + \Delta G_a^{sp}(T) \quad (5)$$

where and $\mathcal{N}$ is the Avogadro's number, ε_0 the permittivity of vacuum, S denoting the solid particle, X the solvent molecule separated by a distance H.

By choosing $\mathcal{P}_{SX} = \frac{\varepsilon_S\,\varepsilon_X}{(\varepsilon_S + \varepsilon_X)}\alpha_{0X}$ as thermodynamic parameter and taking the adsorption of n-alkanes on the solid material, one can write the following equation (6):

$$RTlnVn(n-alkane) = A\left[\frac{3\mathcal{N}}{2(4\pi\varepsilon_0)^2}\mathcal{P}_{SX(n-alkane)}\right] - C \quad (6)$$

where C is an interaction constant of the adsorbed molecule and A is given by:

 doi:10.20944/preprints202401.1548.v1

$$A = \frac{\alpha_{0S}}{H^6} \quad (7)$$

The variations of $RTlnVn(n-alkane)$ as a function of $\frac{3\mathcal{N}}{2(4\pi\varepsilon_0)^2}\mathcal{P}_{SX(n-alkane)}$ gave a straight-line called "n-alkanes straight-line"

In the case of polar molecule X, one deduced the specific or polar free energy of interaction between the adsorbed molecule and the solid surface from equation (8) at a temperature T:

$$\left(-\Delta G_a^{sp}(T)\right) = RTlnVn(X) - A\left[\frac{3\mathcal{N}}{2(4\pi\varepsilon_0)^2}\mathcal{P}_{S-X}\right] + C \quad (8)$$

The determination of $\left(-\Delta G_a^{sp}(T)\right)$ versus the temperature and obtain led to obtain the specific enthalpy $\left(-\Delta H_a^{sp}\right)$ and entropy $\left(-\Delta S_a^{sp}\right)$ of polar solvents, and therefore the Lewis's acid base constants K_A and K_D by using equation (9):

$$\left(-\Delta H^{Sp}\right) = K_A \times DN + K_D \times AN \quad (9)$$

where *AN* and *DN* are respectively the electron donor and acceptor numbers of the polar molecule calculated by Gutmann [45] and corrected by Fowkes [46].

Several organic solvents were used in this study: the n-alkanes composed by n-pentane, n-hexane, n-heptane and n-octane whereas the polar probes were the following: Lewis's acid such as dichloromethane, basic such as ethyl acetate, diethyl ether, tetrahydrofuran and amphoteric such as acetonitrile. The experimental conditions of IGC technique were identical to those given in previous published papers [32–35].

3. Experimental results

3.1. Polar surface interactions between solid materials and organic molecules

On Table 1, one gave the different values of α_{0X} and $\mathcal{P}_{SX}$ of the various organic solvents and their ionization energy obtained from the Handbook of Physics and Chemistry [47].

Table 1. Values of deformation polarizability (in 10^{-30} m^3) and (in 10^{-40} C m^2/V) and ionization energy (in eV) of the various molecules.

Molecule	ε_X (eV)	α_0 (in 10^{-30} m^3)	α_0 (in 10^{-40} C m^2/V)
n-pentane	10.28	9.99	11.12
n-hexane	10.13	11.90	13.24
n-heptane	9.93	13.61	15.14
n-octane	9.80	15.90	17.69
CH_2Cl_2	11.32	7.21	8.02
Diethyl ether	9.51	9.47	10.54
Tetrahydrofuran	9.38	8.22	9.15
Ethyl acetate	10.01	9.16	10.19
Acetonitrile	12.20	4.44	4.94
TAPPy-TPA-COF	7.88	22.38	24.9

The values of the harmonic mean of ionization energies and parameter $\frac{3\mathcal{N}}{2(4\pi\varepsilon_0)^2}\mathcal{P}_{S-X}$ were presented on Table 2.

 doi:10.20944/preprints202401.1548.v1

Table 2. Values of the harmonic mean of the ionization energies $\frac{\varepsilon_S\,\varepsilon_X}{(\varepsilon_S+\varepsilon_X)}$ of TAPPy-TPA-COFs and organic solvents (in 10^{-19} J) and the parameter $\frac{3\mathcal{N}}{2(4\pi\varepsilon_0)^2}\mathcal{P}_{S-X}$ (in 10^{-15} SI unit) for the various organic molecules.

Molecule	$\frac{\varepsilon_S\,\varepsilon_X}{(\varepsilon_S+\varepsilon_X)}$ (in 10^{-19}J)	$\frac{3\mathcal{N}}{2(4\pi\varepsilon_0)^2}\mathcal{P}_{S-X}$ (in 10^{-15} SI)
n-pentane	7.137	57.886
n-hexane	7.092	68.513
n-heptane	7.030	77.674
n-octane	6.989	90.213
CH_2Cl_2	7.433	43.512
Diethyl ether	6.895	53.010
Tetrahydrofuran	6.852	45.726
Ethyl acetate	7.055	52.462
Acetonitrile	7.660	27.613

By using the values presented on Tables 1 and 2, one obtained the values of the polar free surface energy ($-\Delta G_a^{sp}(T)$) of the polar solvents adsorbed on single-crystalline and poly-crystalline TAPPy-TPA-COFs as a function of the temperature T. On gave the obtained results on Table 3.

Table 3. Values of ($-\Delta G_a^{sp}(T)$) (in kJ/mol) of polar molecules adsorbed on single-crystalline and polycrystalline TAPPy-TPA-COFs.

Single-crystalline TAPPy-TPA-COFs				
T(K)	393.15	403.15	413.15	423.15
CH_2Cl_2	2.161	2.036	1.719	1.691
Diethyl ether	1.343	1.229	0.966	1.043
THF	5.031	4.879	4.565	4.385
Ethyl Acetate	4.149	3.925	3.683	3.580
Acetonitrile	6.794	6.364	6.069	5.702
Polycrystalline TAPPy-TPA-COFs				
T(K)	393.15	403.15	413.15	423.15
CH_2Cl_2	3.317	3.019	3.382	2.998
Diethyl ether	2.245	2.049	1.805	2.024
THF	6.463	5.978	6.302	5.824
Ethyl Acetate	6.058	5.685	5.788	5.443
Acetonitrile	11.426	10.550	10.899	9.892

The values given on Table 3 showed that the polycrystalline TAPPy-TPA-COFs exhibited higher acid-base interactions than single-crystalline TAPPy-TPA-COFs for all polar solvents with an increasing amphoteric character.

Now, the polar surface energy of interaction $\gamma_{S-X}^{p}(T)$ reflecting the polarity of the adsorbate X was directly calculated from the values of ($-\Delta G_a^{sp}(T)$) given on Table 3 by using the values of the surface areas of polar molecules as a function of the temperature given by Hamieh thermal model [32–37]. The obtained results for the two COFs were presented on Table 4.

 doi:10.20944/preprints202401.1548.v1

Table 4. Values of polar surface energy of interaction $\gamma_{S-X}^{p}(T)$ (in mJ/m²) of polar molecules adsorbed on single-crystalline and polycrystalline TAPPy-TPA-COFs.

Single-crystalline TAPPy-TPA-COFs				
T(K)	393.15	403.15	413.15	423.15
CH_2Cl_2	8.1	7.5	6.2	6.0
Diethyl ether	4.0	3.6	2.8	3.0
THF	21.0	20.3	18.9	18.1
Ethyl Acetate	13.8	13.0	12.1	11.7
Acetonitrile	20.7	19.2	18.1	16.8
Polycrystalline TAPPy-TPA-COFs				
T(K)	393.15	403.15	413.15	423.15
CH_2Cl_2	12.5	11.1	12.3	10.7
Diethyl ether	6.7	6.0	5.2	5.8
THF	27.0	24.9	26.1	24.0
Ethyl Acetate	20.2	18.8	19.0	17.7
Acetonitrile	34.7	31.8	32.5	29.2

Table 4 showed that the polar surface energy of interaction γ_{S-X}^{p} of polar molecules adsorbed on polycrystalline TAPPy-TPA-COFs is about 1.5 times greater than that of single-crystalline TAPPy-TPA-COFs for the different molecules and at any temperature. A decrease of γ_{S-X}^{p} of the various polar solvents was observed when the temperature increases. The values on Table 4 proved that the largest polar surface interaction was obtained with acetonitrile followed by tetrahydrofuran and ethyl acetate. This is certainly due to the presence of π-electron-rich triple bond that could enhance $\pi-\pi$ interactions between acetonitrile and the two COFs and free pairs of electrons in tetrahydrofuran and ethyl acetate molecules.

3.2. Lewis's acid and base surface energies of COFs

The Van Oss's relation was used to determine the Lewis acid γ_s^+ and base γ_s^- surface energies of the two COFs. Van Oss et al. proposed [48] the following equation:

$$-\Delta G_a^{sp}(T) = 2\mathcal{N}a\left(\sqrt{\gamma_l^-\gamma_s^+} + \sqrt{\gamma_l^+\gamma_s^-}\right) \tag{10}$$

where γ_l^+ and γ_l^- are the respective acid-base contributions of the Lewis base surface energy of the solvent adsorbed on COFs.

The two monopolar solvents used were ethyl acetate (EA) and dichloromethane (CH_2Cl_2) respectively characterized by $\gamma_{EA}^+ = 0\,, \gamma_{EA}^- = 19.2\ mJ/m^2$ and $\gamma_{CH2Cl2}^+ = 5.2\ mJ/m^2\,, \gamma_{CH2Cl2}^- = 0$. This led to the determination of the Lewis's acid and base surface energies of the COFs by using relations (11):

$$\begin{cases} \gamma_s^+ = \dfrac{\left[\Delta G_a^{sp}(T)\ (EA)\right]^2}{4\mathcal{N}^2[a(EA)]^2\gamma_{EA}^-} \\ \gamma_s^- = \dfrac{\left[\Delta G_a^{sp}(T)\ (CH2Cl2)\right]^2}{4\mathcal{N}^2[a(CH2Cl2)]^2\gamma_{CH2Cl2}^+} \end{cases} \tag{11}$$

The values of $\Delta G_a^{sp}(T)\ (EA)$ and $\Delta G_a^{sp}(T)\ (CH2Cl2)$ as a function of the temperature are given by Table 3, whereas, the surface area $a(EA)$ and $a(CH2Cl2)$ are taken from reference []. Furthermore, the total acid-base surface energy γ_s^{AB} of the two COFs was obtained from relation (12).

$$\gamma_s^{AB} = 2\sqrt{\gamma_s^+\gamma_s^-} \tag{12}$$

 doi:10.20944/preprints202401.1548.v1

Relations (11) and (12) allowed to determine the values of γ_s^+, γ_s^- and γ_s^{AB} of single-crystalline and polycrystalline TAPPy-TPA-COFs. The results were given on Table 5.

Table 5. Values of the polar acid and base surface energies γ_s^+, γ_s^- and γ_s^{AB} (in mJ/m²) of single-crystalline and polycrystalline TAPPy-TPA-COFs.

In mJ/m²	Single-crystalline TAPPy-TPA-COF			Polycrystalline TAPPy-TPA-COF		
T(K)	γ_s^-	γ_s^+	γ_s^{AB}	γ_s^-	γ_s^+	γ_s^{AB}
393.15	2.54	2.07	4.59	7.46	4.42	11.48
403.15	2.21	1.82	4.01	6.37	3.81	9.85
413.15	1.55	1.57	3.11	5.33	3.50	8.63
423.15	1.46	1.45	2.92	4.38	3.19	7.47

Table 5 showed that the highest values of the polar acid and base surface energies were obtained for polycrystalline TAPPy-TPA-COF, whereas, those of single-crystalline TAPPy-TPA-COF are very weak proving the non-polar character of this material. This result confirmed that obtained when determining the specific free energy of adsorption on the two COFs and their polar surface energy of interaction $\gamma_{S-X}^p(T)$. One also observed that total acid-base surface energy γ_s^{AB} of polycrystalline TAPPy-TPA-COF is 5 times larger than that of single-crystalline TAPPy-TPA-COF with more accentuated value of the basic surface energy γ_s^-. However, one found approximately identical values for the acid surface energy of materials. It was observed a decrease of the different acid-base components of COFs when the temperature increases.

By using our thermal model, one determined the values of the dispersive component of the surface energy of the two COF materials as a function of the temperature. These values were given on Table 6. The values of γ_s^{AB} from Table 5 allowed to obtain the total surface energy γ_s^{LW} also called Lifshitz – Van der Waals (LW) surface energy of single-crystalline and polycrystalline TAPPy-TPA-COFs by using relation (13).

$$\gamma_s^{LW} = \gamma_s^d + \gamma_s^{AB} \tag{13}$$

Table 6. Values of the dispersive γ_s^d and total γ_s^{tot} surface energies (in mJ/m²) of single-crystalline and polycrystalline TAPPy-TPA-COFs.

In mJ/m²	Single-crystalline TAPPy-TPA-COF		Polycrystalline TAPPy-TPA-COF	
T(K)	γ_s^d	γ_s^{LW}	γ_s^d	γ_s^{LW}
393.15	66.23	70.82	93.80	105.28
403.15	56.47	60.48	78.18	88.03
413.15	47.47	50.59	69.38	78.01
423.15	38.84	41.75	52.03	59.50

The results of Table 6 showed that the polycrystalline TAPPy-TPA-COF surface exhibited higher dispersive, polar and total surface energies about 1.5 times greater than those of the single-crystalline TAPPy-TPA-COF material.

3.3. Lewis's acid-base parameters

The values of $\Delta G_a^{sp}(T)$ of the various polar molecules given on Table 3 as a function of the temperature allowed to obtain their polar or specific enthalpy $(-\Delta H_a^{sp})$ and entropy $(-\Delta S_a^{sp})$ of adsorption on the two COFs. Table 7 gave the obtained results.

Table 7. Values of $(-\Delta H_a^{sp}\ in\ kJ\ mol^{-1})$ and $(-\Delta S_a^{sp} in\ J\ K^{-1} mol^{-1})$ of adsorption on the single-crystalline and polycrystalline TAPPy-TPA-COFs.

Single-crystalline TAPPy-TPA-COF

 doi:10.20944/preprints202401.1548.v1

Polar solvent	$(-\Delta S_a^{sp} in\ J\ K^{-1}mol^{-1})$	$(-\Delta H_a^{sp}\ in\ kJ\ mol^{-1})$
CH_2Cl_2	22.1	10.868
Diethyl ether	18.9	8.7816
THF	22.5	13.906
Ethyl acetate	19.5	11.792
Acetonitrile	35.7	20.819
Polycrystalline TAPPy-TPA-COF		
Polar solvent	$(-\Delta S_a^{sp} in\ J\ K^{-1}mol^{-1})$	$(-\Delta H_a^{sp}\ in\ kJ\ mol^{-1})$
CH_2Cl_2	21.4	11.756
Diethyl ether	22	10.899
THF	35.6	20.404
Ethyl acetate	24.5	15.652
Acetonitrile	59.6	34.712

The previous results concerning the polarity of the two studied COFs were here confirmed by the values on Table 7 of the polar enthalpy of adsorption of the polar solvents. One observed that all values of $(-\Delta H_a^{sp})$ of adsorption on the polycrystalline TAPPy-TPA-COF were greater than the single-crystalline TAPPy-TPA-COF.

In order to better understand the Lewis acid-base behavior of the two COF surfaces, one determined the acid-base parameters following equation (9) and results on Table 7. On Figure 1, one plotted the variations $\left(\frac{-\Delta H_a^{sp}}{AN'}\right)$ as a function of $\left(\frac{DN'}{AN'}\right)$ of polar molecules adsorbed on the two COFs. The straight-line obtained exhibited two different slopes showing a difference between the Lewis acid-base constants of the studied materials and especially larger acidic constant for polycrystalline surface. The obtained results were given on Table 8.

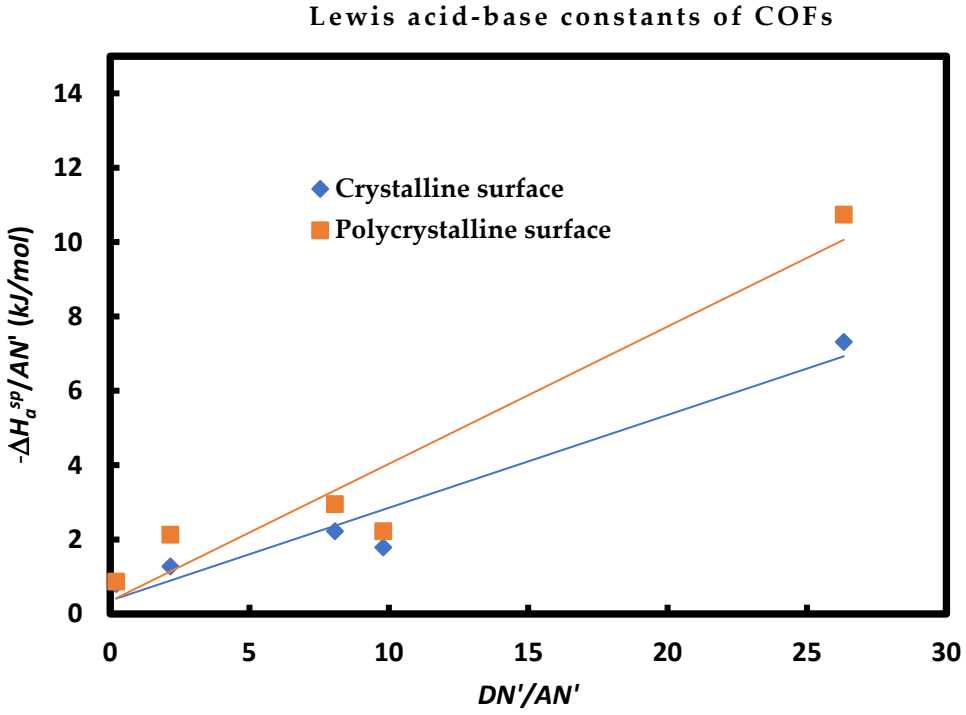

Figure 1. Variations of $\left(\frac{-\Delta H_a^{sp}}{AN'}\right)$ as a function of $\left(\frac{DN'}{AN'}\right)$ of polar molecules adsorbed on crystalline and polycrystalline surfaces.

 doi:10.20944/preprints202401.1548.v1

Table 8. Values of the enthalpic acid base constants K_A and K_D and the entropic acid base constants ω_A and ω_D of the single-crystalline and polycrystalline TAPPy-TPA-COFs with their corresponding acid base ratios and linear regression coefficients.

COF surfaces	K_A	K_D	K_D/K_A	R^2	$10^3.\omega_A$	$10^3.\omega_D$	ω_D / ω_A	R^2
Single-crystalline COF	0.149	0.213	1.430	0.947	0.236	0.570	2.413	0.9724
Polycrystalline COF	0.221	0.205	0.930	0.924	0.386	0.358	0.928	0.9361

Table 8 clearly showed the Lewis amphoteric character of the single and polycrystalline COFs with a greater Lewis basicity for the single-crystalline TAPPy-TPA-COF surface and greater Lewis acidity for the polycrystalline TAPPy-TPA-COF surface. It was also observed that $\frac{K_A(Polycrystalline\ COF)}{K_A(Single-crystalline\ COF)} = 1.48$ and $\frac{K_D(Polycrystalline\ COF)}{K_D(Single-crystalline\ COF)} = 0.96$ that the polycrystalline COF surface was more acidic than the single-crystalline COF surface, whereas, their basicity was comparable. The same results were confirmed by the Lewis entropic acid-base parameters.

The obtained results of the Lewis acid-base constants of the two COFs one again confirmed those obtained for the polar enthalpy and acid-base surface energies of the single and polycrystalline surfaces.

3.4. Consequences and discussion of the new results on COF surfaces

3.4.1. London dipersiveand polar energies of interaction

The new proposed parameter $\mathcal{P}_{SX} = \frac{\varepsilon_S\,\varepsilon_X}{(\varepsilon_S + \varepsilon_X)}\alpha_{0X}$ allowed a net separation between the London dispersion energy and the polar free energy of the adsorption of polar organic molecules and COF surfaces. The new method quatified the London dipersive energy of interaction for both n-alkanes by suing relation (14)

$$\Delta G_a^d(T) = A\left[\frac{3\mathcal{N}}{2(4\pi\varepsilon_0)^2}\mathcal{P}_{SX}\right] \qquad (14)$$

By applying relation (14), one obtained both the London dispersive and polar free energies of all solvents. The results of London dispersion interactions were presented on Table 9.

Table 9. Values of London dispersion interactions $(-\Delta G_a^d(T)\ in\ kJ\ mol^{-1})$ of organic molecules adsorbed on single-crystalline and polycrystalline TAPPy-TPA-COFs.

Single-crystalline TAPPy-TPA-COF				
T(K)	**393.15**	**403.15**	**413.15**	**423.15**
n-pentane	19.861	19.073	18.431	17.962
n-hexane	23.507	22.575	21.815	21.260
n-heptane	26.650	25.593	24.731	24.102
n-octane	30.952	29.725	28.724	27.993
CH_2Cl_2	14.929	14.337	13.854	13.502
Diethyl ether	18.188	17.467	16.878	16.449
Tetrahydrofuran	15.689	15.067	14.559	14.189
Ethyl acetate	18.000	17.286	16.704	16.279
Acetonitrile	9.474	9.098	8.792	8.568
Polycrystalline TAPPy-TPA-COF				
T(K)	**393.15**	**403.15**	**413.15**	**423.15**
n-pentane	23.664	22.471	22.298	20.793
n-hexane	28.008	26.597	26.391	24.610
n-heptane	31.753	30.153	29.920	27.900

 doi:10.20944/preprints202401.1548.v1

n-octane	36.879	35.021	34.750	32.405
CH_2Cl_2	17.788	16.891	16.761	15.630
Diethyl ether	21.671	20.579	20.420	19.041
Tetrahydrofuran	18.693	17.751	17.614	16.425
Ethyl acetate	21.447	20.366	20.209	18.845
Acetonitrile	11.288	10.719	10.636	9.918

Table 9 also showed the higher values of the London dispersion inetractions of the polycrystalline TAPPy-TPA-COF than those obtained with the single-crystalline e TAPPy-TPA-COF for all used organic molecules and all temperatures. The results of Table 9 allowed to obtain the London dispersive enthalpy and entropy of interaction for the two COFs. The obtained values were given on Table 10.

Table 10. Values of Values of London dispersion entropy ($-\Delta S_a^d in\ J\ K^{-1}mol^{-1}$) and enthalpy($-\Delta H_a^d\ in\ kJ\ mol^{-1}$) of organic molecules adsorbed on single-crystalline and polycrystalline TAPPy-TPA-COF surfaces.

COF surfaces	**Single-crystalline TAPPy-TPA-COF**		**Polycrystalline TAPPy-TPA-COF**	
Dispersion parameters	$(-\Delta S_a^d in\ J\ K^{-1}mol^{-1})$	$(-\Delta H_a^d\ in\ kJ\ mol^{-1})$	$(-\Delta S_a^d in\ J\ K^{-1}mol^{-1})$	$(-\Delta H_a^d\ in\ kJ\ mol^{-1})$
n-pentane	63.4	44.702	87.9	58.171
n-hexane	75	52.909	104	68.85
n-heptane	85.1	59.983	117.9	78.056
n-octane	98.8	69.667	136.9	90.657
CH_2Cl_2	47.6	33.602	66.1	43.726
Diethyl ether	58	40.937	80.5	53.271
Tetrahydrofuran	50.1	35.312	69.4	45.951
Ethyl acetate	57.4	40.514	79.6	52.721
Acetonitrile	30.2	21.324	41.9	27.749

One observed that the values of all dispersive and polar parameters of polycrystalline TAPPy-TPA-COF surface were greater than that of single-crystalline TAPPy-TPA-COF surface.

The results on Table 10 allowed to draw on Figure 2 the variations of London dispersion enthalpie $(-\Delta H_a^d)$ as a function of London dispersion entropy $(-\Delta S_a^d)$ for the two COFs and the variations corresponding to polar or specific variables of adsorption. A perfect linearity (with R^2= 1) was observed. The obtained straight lines werere given below.

In the case of single-crystalline TAPPy-TPA-COF (SC) one obtained equation (15), whereas equation (16) was given for polycrystalline TAPPy-TPA-COF (PC) and

$$(-\Delta H_a^d\ in\ kJ\ mol^{-1})\ (SC) = 0.7046\ (-\Delta S_a^d in\ J\ K^{-1}mol^{-1})(SC) + 0.0501 \quad (15)$$

$$(-\Delta H_a^d\ in\ kJ\ mol^{-1})\ (PC) = 0.6622\ (-\Delta S_a^d in\ J\ K^{-1}mol^{-1})(PC) - 0.0201 \quad (16)$$

On also drew on Figure 1 the evolution the specific enthalpy as a function of the specific entropy and obtained the following equations:

$$(-\Delta H_a^{sp}\ in\ kJ\ mol^{-1})\ (SC) = 0.643.6\ (-\Delta S_a^{sp} in\ J\ K^{-1}mol^{-1})(SC) - 2.0455 \quad (17)$$

$$(-\Delta H_a^{sp}\ in\ kJ\ mol^{-1})\ (PC) = 0.5978\ (-\Delta S_a^{sp} in\ J\ K^{-1}mol^{-1})(PC) - 0.8168 \quad (18)$$

These results conducted us to propose in both cases of dispersion and polar enthalpies and entropies the general equations (19) and (20) relative to the respective dispersion and polar cases:

$$(-\Delta H_a^d)\ (X) = T_S^d(-\Delta S_a^d)(X) + (-\Delta G_a^d(S)) \quad (19)$$

$$(-\Delta H_a^{sp})\ (X) = T_S^d(-\Delta S_a^{sp})(X) + (-\Delta G_a^{sp}(S)) \quad (20)$$

 doi:10.20944/preprints202401.1548.v1

*w*here T_S^d and $(-\Delta G_a^d(S))$ are two new characteritics of solid substrate respectively representing a dispersion temperature and free dispersion energy of the solid and T_S^{sp} and $(-\Delta G_a^{sp}(S))$ those corresponding to the polar interation of the solid. One deduced that every solid surface can be charcterized by two dispersion parameters T_S^d and $(-\Delta G_a^d(S))$ and two ploar parameters T_S^{sp} and $(-\Delta G_a^{sp}(S))$.

By combining the two dispersion and polar effects, one obtained the following relations:

$$(-\Delta H_a^{d,sp}\ in\ kJ\ mol^{-1})\ (SC) = 0.7553\ (-\Delta S_a^{d,sp} in\ J\ K^{-1}mol^{-1})(SC) - 3.6943 \quad (21)$$

$$(-\Delta H_a^{d,sp}\ in\ kJ\ mol^{-1})\ (PC) = 0.6879\ (-\Delta S_a^{d,sp} in\ J\ K^{-1}mol^{-1})(PC) - 2.7881 \quad (22)$$

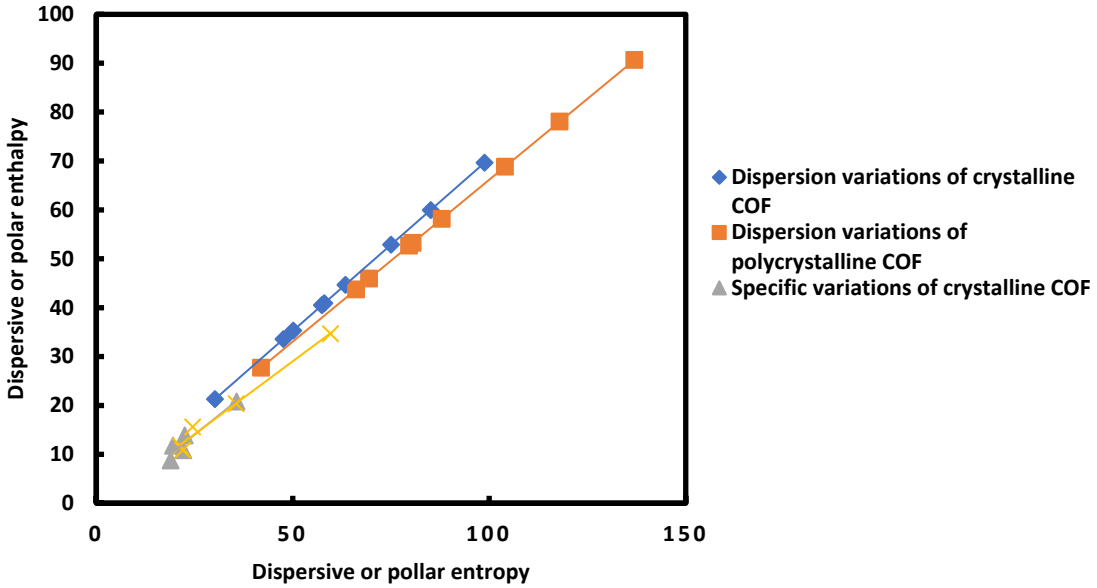

Figure 2. Variations of London dispersion enthalpie $(-\Delta H_a^{d}\ in\ kJ\ mol^{-1})$ as a function of London dispersion entropy $(-\Delta S_a^{d} in\ J\ K^{-1}mol^{-1})$ for the two COFs and the variations corresponding to polar or specific variables $(-\Delta H_a^{sp}\ in\ kJ\ mol^{-1})$ and $(-\Delta S_a^{sp} in\ J\ K^{-1}mol^{-1})$ of adsorption.

Table 10 and Figure 2 led to give the results of Table 11 these four characteristics for the two COFS.

Table 11. Values of the new characteristics of single-crystalline and polycrystalline TAPPy-TPA-COF surfaces. These values were directly deduced from relations (15) to (22).

COF surfaces	Single-crystalline TAPPy-TPA-COF	Polycrystalline TAPPy-TPA-COF
T_S^d (K)	704.6	662.2
T_S^{sp} (K)	643.6	597.8
$(-\Delta G_a^d(S))$ (J/mol)	-50.1	20.1
$(-\Delta G_a^{sp}(S))$ (J/mol)	2046	817
T_S (K)	755.3	687.9
$(-\Delta G_a(S))$ (J/mol)	3694	2788

These new findings deserve more reflection and deepening. One observed that the dispersion temperature is less than the polar temperature for the two COFs. However, the dispersion temperature is greater in the case of single-crystalline COF. The same result was obtained with the polar temperature. One gave on Table 11 the values of the intrinsic temperature T_S and free energy $(-\Delta G_a(S))$ of the materials. One found that that $T_S(SC) = 755.3\ K$ and $T_S(PC) = 687.9K$ showing that the higher intrinsic temperature was obtained by the single-crystalline COF with a difference

 doi:10.20944/preprints202401.1548.v1

between the two temperatures equal to 67.4K. These values will be probably related to the melting point or decomposition temperature of materials.

3.4.2. Comparison with the values obtained by using Donnet et al. method [27]

In order to comapre between our results and those obtained when using Donnet et al. method [27], one gave on Table 12 the values of specific free energy of polar solvents adsorbed on single-crystalline and polycrystalline surfaces.

Table 12. Values of $(-\Delta G_a^{sp}(T))$ (in kJ/mol), $(-\Delta S_a^{sp} in\ J\ K^{-1}mol^{-1})$ and $(-\Delta H_a^{sp} in\ kJ\ mol^{-1})$ of polar molecules adsorbed on single-crystalline and polycrystalline TAPPy-TPA-COFs by using Donnet et al. method [27].

Single-crystalline surface						
T(K)	393.15	403.15	413.15	423.15	$(-\Delta S_a^{sp} in\ J\ K^{-1}mol^{-1})$	$(-\Delta H_a^{sp} in\ kJ\ mol^{-1})$
CH_2Cl_2	-6.994	-6.753	-6.774	-6.586	-12	-11.684
Diethyl ether	2.422	2.268	1.970	2.023	14.9	8.2649
THF	5.271	5.114	4.791	4.607	23.1	14.385
Ethyl Acetate	3.047	2.871	2.663	2.587	15.9	9.2637
Acetonitrile	7.794	7.329	7.001	6.613	38.7	22.982
Polycrystalline surface						
T(K)	393.15	403.15	413.15	423.15	$(-\Delta S_a^{sp} in\ J\ K^{-1}mol^{-1})$	$(-\Delta H_a^{sp} in\ kJ\ mol^{-1})$
CH_2Cl_2	-7.589	-7.334	-6.894	-6.584	-34.6	-21.202
Diethyl ether	3.527	3.272	3.016	3.154	13.7	8.8457
THF	6.744	6.251	6.571	6.076	16.9	13.286
Ethyl Acetate	4.743	4.441	4.551	4.291	12.5	9.5951
Acetonitrile	12.608	11.680	12.019	10.938	46.7	30.864

The comparison between our results and those obtained by using Donnet et al. method [27] (Tables 3 and 12) showed very large difference due to the insufficiency of the approach proposed by Donnet et al. [27] that neglected the role of the harmonic mean of the ionization energies of organic molecules and solid surface. One observed that the results on Table 12 clearly showed a large difference between the values obtained by the $\frac{(-\Delta G_a^{sp}(Donnet\ et\ al.)}{(-\Delta G_a^{sp}(Hamieh))}$ reaches for some polar molecules 1.7. Furthermore, a negative value of the specific free energy of dichloromethane was obtained by Donnet et al. method. This negative value of $(-\Delta G_a^{sp}(T))$ cannot be acceptable for polar molecule. This resulted from the large approximation used by Donnet et al. two above methods. The same observations was showed for the ratios $\frac{(-\Delta S_a^{sp}(Donnet\ et\ al.)}{(-\Delta S_a^{sp}(Hamieh))}$ and $\frac{(-\Delta H_a^{sp}(Donnet\ et\ al.)}{(-\Delta H_a^{sp}(Hamieh))}$ that varied from 0.6 to 0.8 with also negative values when using Donnet method. These results led to acid-base parameters from Donnet al. method completely different from our new approach. Negative values were also obtained for the Lewis baisc constant by using Donnet al. method [27] showing the non-validity of Donnet et al. approach in this case.

3.4.3. Approximative evaluation of the separation distance H between particles

By using the new proposed method, we were able to determine the average separation distance H between the solid particle and the organic moolecule as a function of the temperature. Our results were given on Table 13.

Table 13. Values of the average separation distance H (in Å) btween the two solid substrates and the organic molecules at different temperatures.

 doi:10.20944/preprints202401.1548.v1

T(K)	393.15	403.15	413.15	423.15
Crystalline surface	6.34	6.39	6.42	6.45
Polycrystalline surface	6.16	6.22	6.22	6.30

One observed that the average separation distance H weakly varied as a function of the temperature and it is approximately the same for the two COF materials with a distance H comprised between 6.2 and 6.4 Å.

Furthermore, the total potential energy of interaction $I_{Tot.}(r)$ between a solid particle and an organic molecule, separated by a distance r, is equal to the sum of the repulsive $I_{Rep.}(r)$ and Van der Waals attractive $I_{VDW}(r)$ energies with their respective interaction constants $A_{Rep.}$ and A_{VDW}:

$$I_{Tot.}(r) = I_{Rep.}(r) + I_{VDW}(r) \quad (23)$$

The expressions of $I_{Rep.}(r)$ and $I_{VDW}(r)$ are respectively given by:

$$I_{Rep.}(r) = \frac{A_{Rep.}}{r^{12}}$$
$$I_{VDW}(r) = -\frac{A_{VDW}}{r^{6}} \quad (24)$$

And $I_{Tot.}(r)$ be then written by the Lennard-Jones equation:

$$I_{Tot.}(r) = \frac{A_{Rep.}}{r^{12}} - \frac{A_{VDW}}{r^{6}} \quad (25)$$

The total potential energy of interaction $I_{Tot.}(r)$ is cancelled for r_0 equal to:

$$r_0 = \left(\frac{A_{Rep.}}{A_{VDW}}\right)^{1/6} \quad (26)$$

Whereas, $I_{Tot.}(r)$ reaches its minimum energy for a minimal distance H given by:

$$H = r_{min.} = \left(2\frac{A_{Rep.}}{A_{VDW}}\right)^{1/6} \quad (27)$$

One obtained relation (28):

$$\boldsymbol{r_0 = \frac{H}{2^{1/6}} \approx 0.891H} \quad (28)$$

This allowed to present the obtained results on Table 14.

Table 14. Values of $\boldsymbol{r_0}(in$ Å$)$ and the ratio $A_{Rep.}/A_{VDW}$ $(in$ Å$^6)$ at different temperatures.

TAPPy-TPA-COFS	Crystalline surface		Polycrystalline surface	
T(K)	$\boldsymbol{r_0}$	$A_{Rep.}/A_{VDW}$	$\boldsymbol{r_0}$	$A_{Rep.}/A_{VDW}$
393.15	5.65	1.335	5.49	1.328
403.15	5.69	1.336	5.54	1.330
413.15	5.72	1.337	5.54	1.330
423.15	5.75	1.338	5.61	1.333
Average values	5.70	1.34	5.55	1.33

Table 14 showed a sleight variation of r_0 and the ratio $\boldsymbol{A_{Rep.}/A_{VDW}}$ when the temperature varies. One observed a weak decrease of these parameters in the case of polycrystalline surface.

4. Conclusions

The London dispersive and polar surface thermodynamic parameters of single-crystalline and polycrystalline TAPPy-TPA-COFs were determined by inverse gas chromatography technique (IGC) at infinite dilution. One proposed a new method for the separation of London dispersive and polar surface energies. A new intrinsic thermodynamic parameter $\mathcal{P}_{SX} = \frac{\varepsilon_S \varepsilon_X}{(\varepsilon_S + \varepsilon_X)}\alpha_{0X}$ associating the deformation polarizability of molecules to the harmonic mean of the ionization energies of solid surface and

organic molecules. From the measurements of the net retention volume of the adsorbed solvents on COF surfaces, the use of the new parameter $\mathcal{P}_{SX}$ and by varying the temperature, one obtained the polar interaction energy $\Delta G_a^{sp}(T)$ of the different polar molecules adsorbed on the crystalline and polycrystalline surfaces. This allowed to determine the different components γ_s^+, γ_s^-, γ_s^{AB} of acid-base surface energies of solid surfaces and their total surface energy $\gamma_s^{tot.}$.

One showed that all polar or specific surface parameters of the crystalline COF surface were higher than those obtained with the single-crystalline surface. One observed an excellent linearity of $\left(\frac{-\Delta H_a^{sp}}{AN'}\right)$ versus $\left(\frac{DN'}{AN'}\right)$ of polar molecules adsorbed on crystalline and polycrystalline surfaces allowing the accurate determination of Lewis's acid-base constants. The acidity of the polycrystalline surface was proved to be 1.5 times higher than that of the single-crystalline surface.

This new method allowed to determine the dispersive and specific enthalpy and entropy of adsorption, in both cases of single-crystalline (SC) and polycrystalline (PC) and proved that:

$$(-\Delta H_a^{d,sp})\,(X) = T_S(-\Delta S_a^{d,sp})(X) + (-\Delta G_a^{d,sp}(S))$$

Two new characteritics of solid substrate T_S and $(-\Delta G_a^{d,sp}(S))$ are respectively representing the interaction temperature and free intreaction energy of the solid. One found that that $T_S(SC) = 755.3K$ and $T_S(PC) = 687.9K$ showing that the higher intrinsic temperature was obtained by the single-crystalline COF with a difference between the two temperatures equal to 67.4K. These values will be probably related to the melting point or decomposition temperature of materials. This result has to be confirmed with other solid surfaces in future studies.

The comparison of our results with those obtained by Donnet method showed very large difference in the calculations of the specific or polar surface interactions. This resulted from the fact that Donnet method neglected the effect of the harmonic mean of the ionization energies on the different surface thermodynamic parameters.

These new results also allowed to determine an average value of the separation distance between the COF surfaces and the orgnaic molecules.

Funding: This research did not receive any specific grant.

Data Availability Statement: There is no additional data.

Conflicts of Interest: The author declares no conflict of interest.

References

1. Côté, A. P.; Benin, A. I.; Ockwig, N. W.; O'Keeffe, M.; Matzger, A. J.; Yaghi, O. M. Porous, Crystalline, Covalent Organic Frameworks. *Science* **2005**, *310* (5751), 1166– 1170, DOI: 10.1126/science.1120411
2. Yongqiang Shi, Jinglun Yang, Feng Gao, Qichun Zhang, Covalent Organic Frameworks: Recent Progress in Biomedical Applications, *ACS Nano* 2023, 17, 3, 1879–1905, https://doi.org/10.1021/acsnano.2c11346
3. Ding, S.-Y.; Gao, J.; Wang, Q.; Zhang, Y.; Song, W.-G.; Su, C.-Y.; Wang, W. Construction of Covalent Organic Framework for Catalysis: Pd/COF-LZU1 in Suzuki-Miyaura Coupling Reaction. *J. Am. Chem. Soc.* **2011**, *133* (49), 19816– 19822, DOI: 10.1021/ja206846p
4. . Sharma, R. K.; Yadav, P.; Yadav, M.; Gupta, R.; Rana, P.; Srivastava, A.; Zbořil, R.; Varma, R. S.; Antonietti, M.; Gawande, M. B. Recent development of covalent organic frameworks (COFs): synthesis and catalytic (organic-electro-photo) applications. *Mater. Horizons* **2020**, *7* (2), 411– 454, DOI: 10.1039/C9MH00856J
5. Wang, X.; Han, X.; Zhang, J.; Wu, X.; Liu, Y.; Cui, Y. Homochiral 2D Porous Covalent Organic Frameworks for Heterogeneous Asymmetric Catalysis. *J. Am. Chem. Soc.* **2016**, *138* (38), 12332– 12335, DOI: 10.1021/jacs.6b07714
6. Fortea-Pérez, F. R.; Mon, M.; Ferrando-Soria, J.; Boronat, M.; Leyva-Pérez, A.; Corma, A.; Herrera, J. M.; Osadchii, D.; Gascon, J.; Armentano, D.; Pardo, E. The MOF-driven synthesis of supported palladium clusters with catalytic activity for carbene-mediated chemistry. *Nat. Mater.* **2017**, *16* (7), 760– 766, DOI: 10.1038/nmat4910
7. Tu, W.; Xu, Y.; Yin, S.; Xu, R. Rational Design of Catalytic Centers in Crystalline Frameworks. *Adv. Mater.* **2018**, *30* (33), 1707582, DOI: 10.1002/adma.201707582
8. Sun, T.; Xie, J.; Guo, W.; Li, D.-S.; Zhang, Q. Covalent-Organic Frameworks: Advanced Organic Electrode Materials for Rechargeable Batteries. *Adv. Energy Mater.* **2020**, *10*, 1904199, DOI: 10.1002/aenm.201904199

9. Tong, Y.; Sun, Z.; Wang, J.; Huang, W.; Zhang, Q. Covalent organic framework containing dual redox centers as an efficient anode in Li-ion batteries. *SmartMat* **2022**, *3* (4), 685– 694, DOI: 10.1002/smm2.1115
10. Zhong, L.; Fang, Z.; Shu, C.; Mo, C.; Chen, X.; Yu, D. Redox Donor-Acceptor Conjugated Microporous Polymers as Ultralong-Lived Organic Anodes for Rechargeable Air Batteries. *Angew. Chem., Int. Ed.* **2021**, *60*, 10164– 10171, DOI: 10.1002/anie.202016746
11. Wang, Z.; Zhang, S.; Chen, Y.; Zhang, Z.; Ma, S. Covalent organic frameworks for separation applications. *Chem. Soc. Rev.* **2020**, *49* (3), 708– 735, DOI: 10.1039/C9CS00827F
12. Xu, S.; Zhang, Q. Recent progress in covalent organic frameworks as light-emitting materials. *Mater. Today Energy* **2021**, *20*, 100635, DOI: 10.1016/j.mtener.2020.100635
13. Guo, B.; Huang, Z.; Shi, Q.; Middha, E.; Xu, S.; Li, L.; Wu, M.; Jiang, J.; Hu, Q.; Fu, Z.; Liu, B. Organic Small Molecule Based Photothermal Agents with Molecular Rotors for Malignant Breast Cancer Therapy. *Adv. Funct. Mater.* **2020**, *30* (5), 1907093, DOI: 10.1002/adfm.201907093
14. Zhao, F.; Liu, H.; Mathe, S. D. R.; Dong, A.; Zhang, J. Covalent Organic Frameworks: From Materials Design to Biomedical Application. *Nanomaterials* **2018**, *8* (1), 15, DOI: 10.3390/nano8010015
15. Giri, A.; Hopkins, P. E. Heat Transfer Mechanisms and Tunable Thermal Conductivity Anisotropy in Two-Dimensional Covalent Organic Frameworks with Adsorbed Gases. *Nano Lett.* 2021, *21*, 6188−6193.
16. Guo, J.; Jiang, D. Covalent Organic Frameworks for Heterogeneous Catalysis: Principle, Current Status, and Challenges. *ACS Cent. Sci.* 2020, *6*, 869−879.
17. X. Fu, Z. Lu, H. Yang, X. Yin, L. Xiao, L. Hou, Imine-based covalent organic framework as photocatalyst for visible-light-induced atom transfer radical polymerization, Journal of Polymer Science, 2021, Volume59, Issue18, 15 September 2021, Pages 2036-2044, https://doi.org/10.1002/pol.20210261
18. Natraj, A.; Ji, W.; Xin, J.; Castano, I.; Burke, D. W.; Evans, A. M.; Strauss, M. J.; Ateia, M.; Hamachi, L. S.; Gianneschi, N. C.; ALOthman, Z. A.; Sun, J.; Yusuf, K.; Dichtel, W. R. Single-Crystalline Imine-Linked Two-Dimensional Covalent Organic Frameworks Separate Benzene and Cyclohexane Efficiently. *J. Am. Chem. Soc.* **2022**, *144*, 19813–19824
19. Yusuf, K.; Natraj, A.; Li, K.; Ateia, M.; Al Othman, Z.A.; Dichtel, W.R. Inverse Gas Chromatography Demonstrates the Crystallinity-Dependent Physicochemical Properties of Two-Dimensional Covalent Organic Framework Stationary Phases, *Chemistry of Materials.* **2023,** *35* (4), 1691-1701, https://doi.org/10.1021/acs.chemmater.2c03448
20. Vardhan, H.; Rummer, G.; Deng, A.; Ma, S. Large-Scale Synthesis of Covalent Organic Frameworks: Challenges and Opportunities. *Membranes* **2023**, *13*, 696. https://doi.org/10.3390/membranes13080696
21. Matsumoto, M., Dasari, R. R., Ji, W., Feriante, C. H., Parker, T. C., Marder, S. R., & Dichtel, W. R. (2017). Rapid, low temperature formation of imine-linked covalent organic frameworks catalyzed by metal triflates. *Journal of the American Chemical Society*, *139*(14), 4999-5002
22. de la Peña Ruigómez, A., Rodríguez-San-Miguel, D., Stylianou, K. C., Cavallini, M., Gentili, D., Liscio, F., ... & Zamora, F. (2015). Direct on-surface patterning of a crystalline laminar covalent organic framework synthesized at room temperature. *Chemistry–A European Journal*, *21*(30), 10666-10670.
23. C. Saint-Flour, E. Papirer, Gas-solid chromatography. A method of measuring surface free energy characteristics of short carbon fibers. 1. Through adsorption isotherms, Ind. Eng. Chem. Prod. Res. Dev., 21 (1982) 337-341, doi: 10.1021/i300006a029.
24. C. Saint-Flour, E. Papirer, Gas-solid chromatography: method of measuring surface free energy characteristics of short fibers. 2. Through retention volumes measured near zero surface coverage, Ind. Eng. Chem. Prod. Res. Dev., 21 (1982) 666-669, doi: 10.1021/i300008a031.
25. C. Saint-Flour and E. Papirer, "Gas-solid chromatography: a quick method of estimating surface free energy variations induced by the treatment of short glass fibers." *Journal of Colloid and Interface Science* 91 (1983): 69-75.
26. J. Schultz, L. Lavielle, C. Martin, The role of the interface in carbon fibre-epoxy composites. J. Adhes., 23 (1987) 45–60
27. J.-B. Donnet, S. Park, H. Balard, Evaluation of specific interactions of solid surfaces by inverse gas chromatography, Chromatographia, 31 (1991) 434–440.
28. E. Brendlé, E. Papirer, A new topological index for molecular probes used in inverse gas chromatography for the surface nanorugosity evaluation, 2. Application for the Evaluation of the Solid Surface Specific Interaction Potential, J. Colloid Interface Sci., 194 (1997) 217–2224.

29. E. Brendlé, E. Papirer, A new topological index for molecular probes used in inverse gas chromatography for the surface nanorugosity evaluation, 1. Method of Evaluation, J. Colloid Interface Sci., 194 (1997) 207–216.
30. D.T. Sawyer, D.J. Brookman. Thermodynamically based gas chromatographic retention index for organic molecules using salt-modified aluminas and porous silica beads, *Anal. Chem*. 1968, 40, 1847-1850. https://doi.org/10.1021/ac60268a015.
31. M.M. Chehimi, E. Pigois-Landureau, Determination of acid–base properties of solid materials by inverse gas chromatography at infinite dilution. A novel empirical method based on the dispersive contribution to the heat of vaporization of probes, J. Mater. Chem., 4 (1994) 741–745.
32. T Hamieh, Study of the temperature effect on the surface area of model organic molecules, the dispersive surface energy and the surface properties of solids by inverse gas chromatography, *J. Chromatogr. A*, 1627 (2020) 461372.
33. T Hamieh, AA Ahmad, T Roques-Carmes, J Toufaily, New approach to determine the surface and interface thermodynamic properties of H-β-zeolite/rhodium catalysts by inverse gas chromatography at infinite dilution, Scientific Reports, 10 (1) (2020) 1-27.
34. T Hamieh, New methodology to study the dispersive component of the surface energy and acid–base properties of silica particles by inverse gas chromatography at infinite dilution, Journal of Chromatographic Science 60 (2) (2022) 126-142, https://doi.org/10.1093/chromsci/bmab066
35. T. Hamieh, New Physicochemical Methodology for the Determination of the Surface Thermodynamic Properties of Solid Particles. *AppliedChem* 2023, *3*(2), 229-255; https://doi.org/10.3390/appliedchem3020015.
36. Hamieh, T.; Schultz, J. New approach to characterise physicochemical properties of solid substrates by inverse gas chromatography at infinite dilution. Some new methods to determine the surface areas of some molecules adsorbed on solid surfaces. *J. Chromatogr. A* **2002**, *969*, 17–47. https://doi.org/10.1016/S0021-9673(02)00368-0.
37. Hamieh, T.; Schultz J. Study of the adsorption of n-alkanes on polyethylene surface - State equations, molecule areas and covered surface fraction, *Comptes Rendus de l'Académie des Sciences, Série IIb* **1996,** 323 (4), 281-289,
38. Conder, J.R.; Locke, D.C.; Purnell, J.H. Concurrent solution and adsorption phenomena in chromatography. *I. J. Phys. Chem.* **1969,** 73, 700-8. https://doi.org/10.1021/j100723a035.
39. Conder, J.R.; Purnell, J.H. Gas chromatography at finite concentrations. Part 2.—A generalized retention theory. *Trans Faraday Soc.* **1968,** 64, 3100–11.
40. Conder, J.R.; Purnell, J.H. Gas chromatography at finite concentrations. Part 3.—Theory of frontal and elution techniques of thermodynamic measurement. *Trans Faraday Soc.* **1969,** 65, 824-38. https://doi.org/10.1039/TF9696500824
41. Voelkel, A. Inverse gas chromatography: characterization of polymers, fibers, modified silicas, and surfactants. *Crit Rev Anal Chem.* **1991**, 22, 411-39. https://doi.org/10.1080/10408349108051641.
42. Hamieh, T. New Progress on London Dispersive Energy, Polar Surface Interactions and Lewis's Acid-Base Properties of Solid Surfaces. *Preprints* **2024**, 2024010638. https://doi.org/10.20944/preprints202401.0638.v1.
43. F. London, The general theory of molecular forces, Trans. Faraday. Soc.,33, (1937), pp. 8-26.
44. Hamieh, T. New methods and Protocols to characterize the surface properties of solid materials, submitted to *Chemistry of Materials*, 2023.
45. V. Gutmann, The Donor-acceptor Approach to Molecular Interactions, Plenum. New York, 1978.
46. Riddle, F. L.; Fowkes, F. M. Spectral shifts in acid-base chemistry. Van der Waals contributions to acceptor numbers, Spectral shifts in acid-base chemistry. 1. van der Waals contributions to acceptor numbers. **1990**, *J. Am. Chem. Soc.*, 112 (9), 3259-3264. https://doi.org/10.1021/ja00165a001.
47. David R. Lide, ed., *CRC Handbook of Chemistry and Physics, Internet Version 2007, (87th Edition), <http:/www.hbcpnetbase.com>,* Taylor and Francis, Boca Raton, FL, 2007.
48. C.J. Van Oss, R.J. Good, M.K. Chaudhury, Additive and nonadditive surface tension components and the interpretation of contact angles, Langmuir, 1988, 4 (4) 884, http:// dx.doi.org/10.1021/la00082a018.